

DESIGN, MODELING AND CHARACTERIZATION OF TRIPLY PERIODIC MINIMAL SURFACE HEAT EXCHANGERS WITH ADDITIVE MANUFACTURING

Hao Peng^{1*}, Feng Gao², and Wenjing Hu³

1. ITAMCO & Atlas3D

2. Dept. of Chemical and Biomolecular Engineering, University of Notre Dame

3. Dept. of Applied and Computational Mathematics and Statistics, University of Notre Dame

*Corresponding author: hpeng@itamco.com

Abstract

Next-generation power plants will generate heated fluids at significantly higher temperatures than current-generation power plants, which challenges the state-of-the-art heat exchanger design. In this study triply periodic minimal surfaces were combined with additive manufacturing for next-generation heat exchanger design. Triply periodic minimal surfaces separate three-dimensional space into two interpenetrating channels, creating high surface area to volume ratios and low hydrodynamic resistance. Parametric design of triply periodic minimal surface heat exchanger is straightforward because they are governed by simple implicit functions with parameters such as periodic length and offset parameter. In this study a design workflow was developed to streamline the design of triply periodic minimal surface heat exchangers and a numerical model was developed to optimize triply periodic minimal surface heat exchanger design for optimal performance. Finally, the optimized triply periodic minimal surface heat exchanger was printed with EOS M290 DMLS machine and the performance was tested by experiment.

Keywords: triply periodic minimal surface, additive manufacturing, heat exchanger, lattice structure

Introduction

1.1 State-of-the-art Heat Exchangers

The most commonly utilized heat exchangers in industrial sectors are shell-and-tube heat exchangers, plate-and-frame heat exchangers, plate-fin heat exchangers and printed circuit heat exchangers [1, 2]. Shell-and-tube heat exchangers consists of a shell with tubes inside it; plate-and-frame heat exchangers consist of a series of corrugated plates supported by a rigid frame; plate-fin heat exchangers consist of side bars, fins, and parting sheets; and printed circuit heat exchangers consist of stacked plates with fine grooves etched into each plate as shown in Fig. 1.

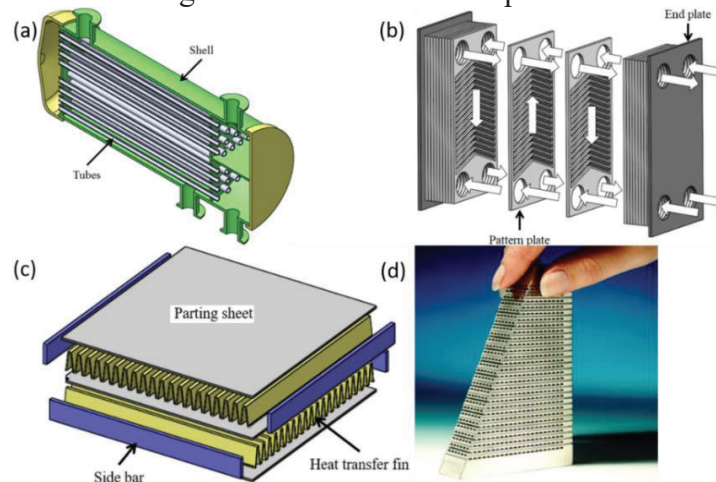


Figure 1. State-of-the-art heat exchangers. (a) shell-and-tube heat exchanger, (b) plate-and-frame heat exchanger, (c) plate-fin heat exchanger and (d) printed circuit heat exchanger [1, 2].

1.2 Heat Exchanger Design Considerations

In design of heat exchangers, following requirements need to be considered [3].

- Operating pressure and temperature. Operating pressure and temperature will influence material choice and can influence designers to select one type of heat exchanger in preference to another.
- Pressure drop. Pressure drop should be in an allowable limit so that free-flow area can meet the design requirement.
- Thermal effectiveness. The thermal effectiveness is determined by heat transfer coefficients and heat transfer surface area.
- Fouling. The heat exchanger design should be free from excessive blockage-causing dirt/particulates/other fouling mechanism.

The comparison of the state-of-the-art heat exchangers in terms of the above design considerations is shown in Table 1. The shell-and-tube heat exchangers offer the highest maximum temperature and pressure. However, they are usually bulky and heavy due to very low surface area to volume ratio, and not economical for high-temperature and high-pressure applications. Plate-and-frame heat exchangers and plate-fin heat exchangers offer higher surface area to volume ratio than shell-and-tube heat exchangers but they are restricted to low or moderate temperature and pressure applications. Besides, pressure drop in those two heat exchangers is relatively high and they are prone to fouling due to narrow passages. Printed circuit heat exchangers achieve high thermal performance and are compact due to the smaller channel geometries. However, they incur larger pressure drops due to long straight micro-channels and they are relatively expensive due to use of chemical etching process [1, 2].

	A_{heat}/V (m^2/m^3)	T_{max} ($^{\circ}C$)	$Pressure_{max}$ (bar)
Shell-and-tube heat exchanger	50 – 100	1100	1000
Plate-and-frame heat exchanger	120 – 660	815	200
Plate-fin heat exchanger	800 – 1500	800	200
Printed circuit heat exchanger	200 – 2500	980	900

Table 1. Comparison of different types of heat exchangers in terms of area-to-volume ratio, maximum operating temperature and pressure [1].

1.3 AM for Heat Exchanger Design

Additive manufacturing (AM), also known as 3D printing, emerged nearly three decades ago [4]. Direct metal laser sintering (DMLS) is an AM process for direct generation of metal components [5]. Components are manufactured directly based on CAD files from metal powder feedstock and built up in a layer-by-layer fashion. The metal powders are locally melted by a high-energy laser and reach almost one hundred percent dense microstructure after solidification without

any additional steps. Thanks to the layer-wise buildup, this process provides components of virtually any shape with almost unlimited freedom of design, and enables manufacturing of complex geometries and internal structures which are not possible with traditional manufacturing techniques. In addition, AM offers almost unlimited freedom of design, and moreover, a variety of materials such as 17-4 stainless steel, Inconel 625 and 718, aluminum AlSi10Mg and titanium Ti6Al4V can be chosen for different applications.

Heat exchangers are a type of components where AM can provide significant advantages in function and efficiency. Figure 2(a) is a multi-furcating heat exchanger designed at General Electric Global Research [1]. The best results showed that the heat exchanger met the pressure drop and heat transfer design requirement with 66% lower weight and 50% lower volume than the conventional heat exchangers. Figure 2(b) shows a heat exchanger with a large number of intricate channels and complex internal structures which are designed to maximize surface area to volume ratio for high efficiency of heat transfer [6]. Figure 2(c) shows a heat exchanger designed and built by EOS® with AM technology. The heat exchanger is self-supporting with integrated cooling fins on outside surfaces [7].

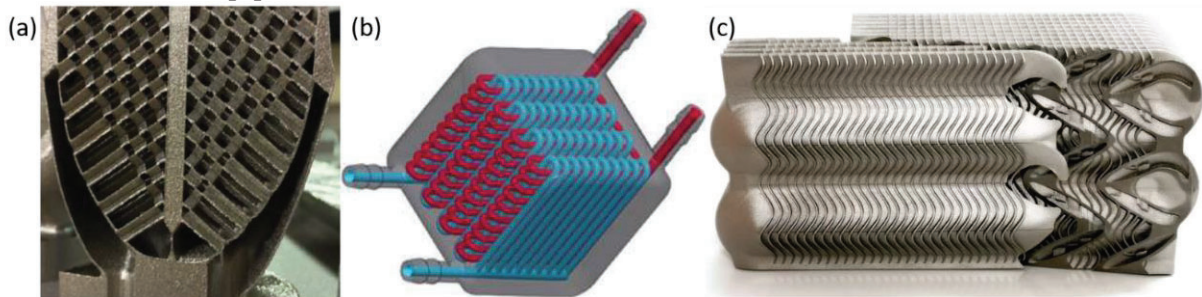


Figure 2. (a) Multi-furcating heat exchanger, (b) heat exchanger design with intricate inner channels, and (c) heat exchanger designed by EOS.

Triply periodic minimal surface heat exchanger (TPMS-HX) is a new type of heat exchanger which is only possible with AM. The concept of applying TPMS to heat and mass transfer devices was first introduced by Slaughter [8] in 2003. The concept was later expanded by Ryan [9] in 2013. Various types of TPMS were discussed including the Schwartz's D surface, Schwartz's P surface, Schoen's Gyroid Surface and others. However, those studies only stay on conceptual level. Recently Nguyen and et al. [10] presented a study on TPMS-HX used in s-CO₂ power cycles. Finite element (FEM) simulation was applied to analyze the flow pattern in a simple Gyroid TPMS structure. It was reported heat transfer was improved by a factor of 10-100 in comparison to micro-channel heat exchangers. Chandrasekaran [11] performed an experimental study on Schwartz's D TPMS-HX. The geometry of the TPMS-HX was a simple cube and the material used was Nylon 12. To the best of the authors' knowledge, existing studies on TPMS-HX are focused on simple cube- or block-type geometries and no metal TPMS-HX is investigated experimentally. This limitation is possibly due to the difficulties of design and manufacturing of complex TPMS-HX geometries by traditional CAD software and manufacturing techniques. In this manuscript, the design, modeling and characterization of an industrial TPMS-HX is presented. The influence of design parameters of TPMS-HX on the performance of fluid flow and heat transfer is studied by simulation and an EOS M290 powder bed fusion AM machine is employed to build the TPMS-HX for performance testing. The structure of this manuscript is arranged as follows. Section 1 discusses the general design consideration of heat exchanger and the use of AM for TPMS-HX. Section 2 introduces the characteristic of TPMS-HX and the design workflow of

TPMS-HX. Section 3 presents the simulation of TPMS-HX with COMSOL Multiphysics®. The fluid pattern and heat transfer efficiency for different types of TPMS-HX is analyzed. Section 4 shows the experimental studies on the proposed TPMS-HX.

Triply Periodic Minimal Surface Heat Exchanger Design

2.1 Triply periodic minimal surface (TPMS)

TPMS is defined as surfaces of zero mean curvature, meaning that the sum of the principal curvatures at each point is zero. TPMS is a surface minimizes its area with a fixed boundary curve. MS has been mathematically created using level-set equations [12]. These equations consist of implicit trigonometric functions that define an isosurface. Classical examples of TPMSs include Schwartz surface, Gyroid surface and Diamond surface which can be characterized with implicit functions as follows [13].

$$\text{Schwartz: } \cos\left(\frac{2\pi}{L}x\right) + \cos\left(\frac{2\pi}{L}y\right) + \cos\left(\frac{2\pi}{L}z\right) = P, \quad (1.1)$$

$$\text{Gyroid: } \cos\left(\frac{2\pi}{L}x\right)\sin\left(\frac{2\pi}{L}y\right) + \cos\left(\frac{2\pi}{L}y\right)\sin\left(\frac{2\pi}{L}z\right) + \cos\left(\frac{2\pi}{L}z\right)\sin\left(\frac{2\pi}{L}x\right) = P, \quad (1.2)$$

$$\begin{aligned} \text{Diamond: } & \sin\left(\frac{2\pi}{L}x\right)\sin\left(\frac{2\pi}{L}y\right)\sin\left(\frac{2\pi}{L}z\right) + \sin\left(\frac{2\pi}{L}x\right)\cos\left(\frac{2\pi}{L}y\right)\cos\left(\frac{2\pi}{L}z\right) \\ & + \cos\left(\frac{2\pi}{L}x\right)\sin\left(\frac{2\pi}{L}y\right)\cos\left(\frac{2\pi}{L}z\right) + \cos\left(\frac{2\pi}{L}x\right)\cos\left(\frac{2\pi}{L}y\right)\sin\left(\frac{2\pi}{L}z\right) = P \end{aligned}, \quad (1.3)$$

where L is the periodic length and P is the offset parameter. Figure 3 shows the three types of TPMSs in one periodic length with zero offset parameter.

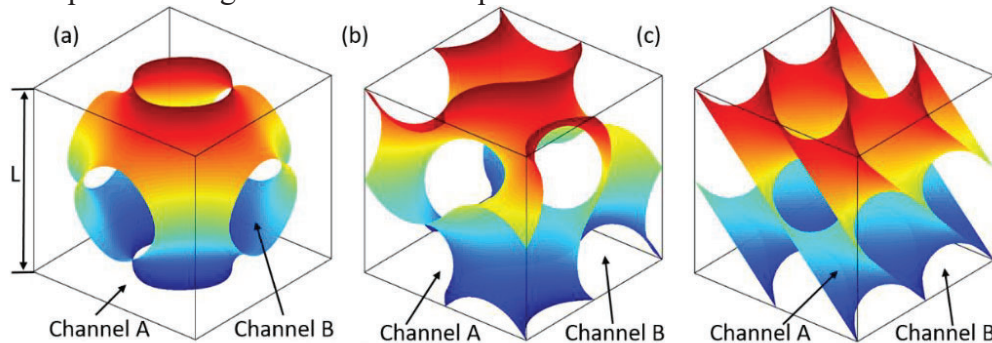


Figure 3. TPMSs in one periodic length: (a) Schwartz surface, (b) Gyroid surface and (c) Diamond surface.

2.2 Characteristics of TPMS

The following unique features of TPMSs make them promising in the next-generation heat exchanger design. (1) TPMSs divide a three-dimensional (3D) domain into two separated but interpenetrating channels which provides large surface area to volume ratio. As such, two flows with different temperatures can pass through the separated channels and exchange heat efficiently. Figure 3 shows how cubic domains are separated into Channel A and Channel B by TPMSs. Figure 4 shows that surface area to volume ratio of a Gyroid triply periodic minimal surface increases exponentially with decreasing periodic length and reaches up to 3000 m²/m³ with periodic length of 1 mm. The surface area can be calculated with

$$S = \iint \sqrt{1 + \left(\frac{\partial z}{\partial x}\right)^2 + \left(\frac{\partial z}{\partial y}\right)^2} dx dy. \quad (2)$$

(2) The mean curvature is zero at any point on a TPMS and each separated channel is interconnected in all directions. Therefore, the flow is free to move in any direction and the hydrodynamic resistance and pressure drop in TPMS is low. (3) TPMSs create complex flow pattern which will enhance heat transfer efficiency and prevent fouling. For example, a helical-fashion flow pattern is generated in a Gyroid TPMS. The vortex in the flow will help increase heat transfer coefficient and prevent fouling by removing dirt or particulates attached to the Gyroid surface. (4) TPMSs exhibit high structural integrity and can realize pressure equalization [8]. TPMS-HX is usually manufactured by AM as a whole piece without welding or brazing. Also, pressure exerted on two sides of a triply periodic minimal surface tends to equalize. Therefore, they can survive demanding working conditions such as high temperature and pressure. (5) TPMSs are governed by simple implicit functions parametric design of TPMS-HX is straightforward. (6) TPMSs are self-supporting structures and the time-consuming support removal process can be avoided after the AM process.

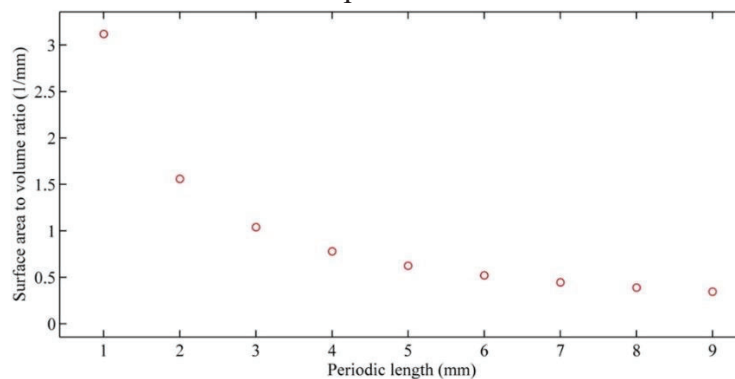


Figure 4. Surface area to volume ratio of a Gyroid surface.

2.3 TPMS-HX Design Considerations

To achieve optimal heat transfer performance, design parameters of TPMS-HX such as type of triply periodic minimal surface, periodic length, wall thickness, triply periodic minimal surface orientation and offset parameter can be adjusted to accommodate various application scenarios.

- ***Type of TPMS:*** The first step in TPMS-HX design is to determine the proper type of triply periodic minimal surface. There are many types of TPMSs and the most classical ones are Schwartz surfaces, Gyroid surfaces and Diamond surface. Because each type of triply periodic minimal surface gives a unique flow pattern, the heat transfer and pressure drop performance will be also different. For example, the Schwartz surface may give a low pressure drop due to its large straight channels along x, y and z direction. However, the heat transfer performance of a Schwartz TPMS-HX may not as good as a Gyroid TPMS-HX because heat transfer in Gyroid surface can be enhanced by its helical-fashion flow pattern. In addition, types of triply periodic minimal surface will influence the manufacturability of TPMS-HX as well as the maximum operating temperature and pressure.
- ***Periodic Length and Wall Thickness:*** The periodic length and wall thickness of TPMS-HX will influence not only the manufacturability but also the heat transfer performance of TPMS-HX. On one hand, the surface area to volume ratio of TPMS-HX increases exponentially with decreasing periodic length as shown by Fig. 4. On the other hand, small periodic length means smaller characteristic dimension which will induce larger pressure

drop. Small wall thickness is desirable for high heat transfer rates but wall thickness should be larger than a threshold value to guarantee a success build in AM.

- Orientation of TPMS: The orientation of TPMSs with respect to flow direction is another influential parameter that needs to be determined. There are a few principal orientations for a TPMS along which straight channels can be observed. For example, Fig. 5 shows two principal orientations of a Gyroid triply periodic minimal surface. The first principal orientation is along the edge direction and the second is along the main diagonal direction. Along principal orientations, flow can easily pass through the straight channels with low pressure drop. However, in some cases, principle orientations should be avoided so that flow can exchange heat sufficiently in TPMS.

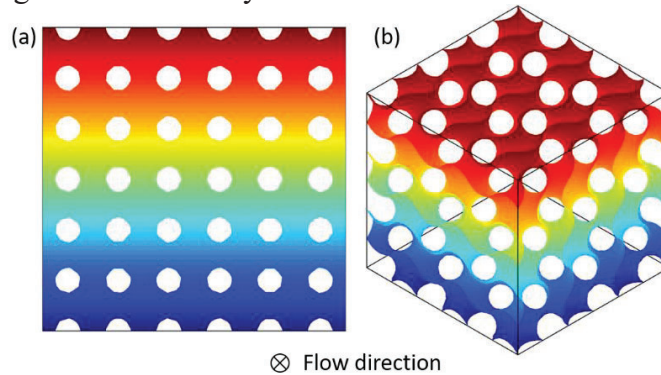


Figure 5. Two principle orientations of Gyroid triply periodic minimal surface structure with respect to flow direction. (a) Flow is along the edge direction. (b) Flow is along the main diagonal direction.

- Offset Parameter of TPMS: The offset parameter in implicit functions of TPMSs will affect the size of two channel separated by the TPMSs. With a zero offset parameter, TPMSs will divide 3D domain equally into two interpenetrating channels. With a nonzero offset, one channel will expand while the other will shrink. Figure 6 shows the Schwartz, Gyroid and Diamond TPMSs with a positive offset parameter of 0.5. Compared to channels shown in Fig. 3, channel A shrinks and channel B expands. TPMS-HX with nonzero offset parameter is especially useful when physical properties of working fluids in the two separated channels are significantly different. For example, flow with higher viscosity can be applied to the expanding channel to reduce hydrodynamic resistance and flow with lower thermal conductivity can be applied to the shrinking channel to enhance heat transfer efficiency.

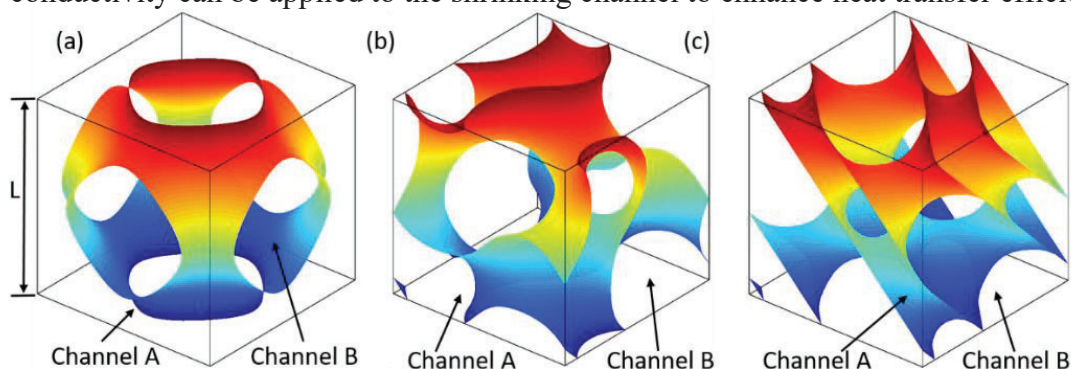


Figure 6. TPMSs with positive offset parameter of 0.5: (a) Schwartz Surface, (b) Gyroid Surface and (c) Diamond Surface.

2.4 Developing CAD Models for TPMS

Some commercial CAD software can generate simple TPMSs but lots of Boolean operations are needed [13]. An alternative approach is to generate TPMSs directly from their implicit functions. In this study, a voxel mesh will be generated for TPMS-HX geometry by evaluating the implicit functions at the center of each voxel. The voxel mesh is converted to STL file by applying the marching cube method. The disadvantage of this approach is that TPMS-HX mesh generated by voxel-based methods is poorly defined at boundaries. This disadvantage can be overcome by reducing the size of the voxel mesh.

Fluid Flow and Heat Transfer in TPMS-HX

3.1 CFD model for TPMS-HX

In this study, a computational fluid dynamics (CFD) model was developed to predict the fluid flow and heat transfer performance of TPMS-HX. Considering that both fluid flow and heat transfer need to be modeled, a multi-physics CFD simulation software COMSOL Multiphysics® is used. The CAD model of TPMS-HX is imported into COMSOL and the conjugate heat transfer module is selected to model the coupled flow and heat transfer physics. Given that flow in TPMS-HX is typically confined in narrow channels and flow velocity is generally much lower than Mach number, flow in TPMS-HX is modeled as laminar and weakly compressible flow. The governing equation for the flow is

$$\rho(\mathbf{u} \cdot \nabla) \mathbf{u} = \nabla \cdot \left[-p\mathbf{I} + \mu(\nabla \mathbf{u} + (\nabla \mathbf{u})^T) - \frac{2}{3} \mu(\nabla \cdot \mathbf{u})\mathbf{I} \right] + \mathbf{F} \quad (3)$$

where \mathbf{u} is flow velocity, ρ is flow density, p is hydrostatic pressure, μ is dynamic viscosity and \mathbf{F} is body force. The heat transfer in TPMS-HX can be modeled by the conjugate heat transfer module in COMSOL. The governing equation is

$$\rho C_p \mathbf{u} \cdot \nabla T + \nabla \cdot (-k \nabla T) = 0 \quad (4)$$

where T is temperature, C_p is specific heat and k is thermal conductivity.

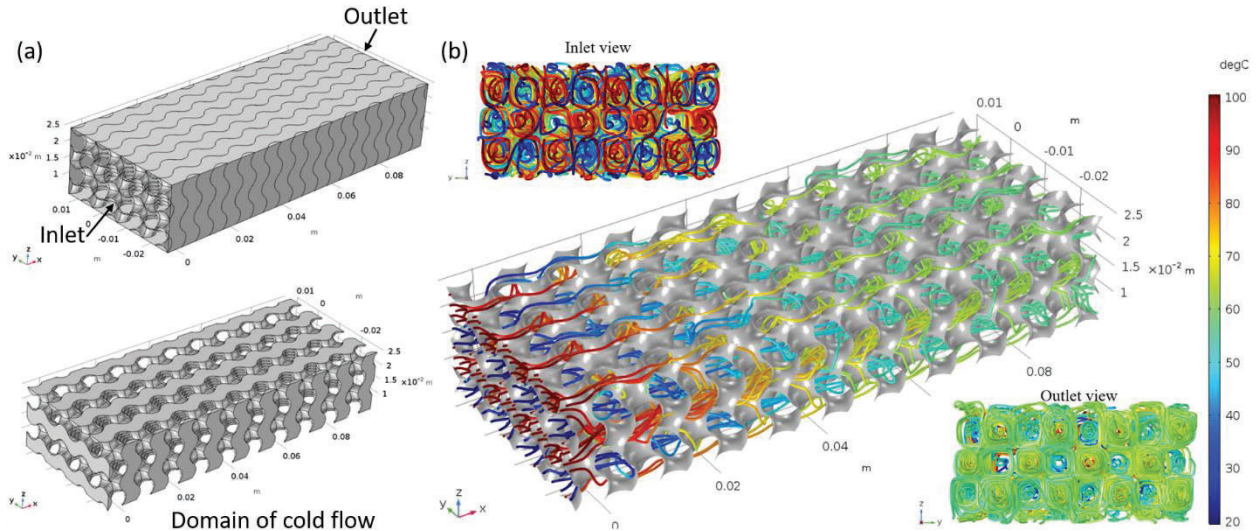


Figure 7. (a) Geometry and boundary condition of a TPMS-HX. (b) Temperature and flow pattern in TPMS-HX.

3.2 Flow pattern in TPMS-HX

Figure 7(a) shows the boundaries, inlets, outlets and flow domains of a TPMS-HX. The periodic length of the TPMS is 10 mm and there are 10, 4 and 2 units along x, y and z direction as shown in Fig. 7(a). Both cold and hot fluids are water and flow in parallel from the inlet end to the outlet end. On the inlet end, the temperatures are 20 °C and 100 °C for the cold and hot fluids, respectively, and fluid velocity is 10 mm/s at the inlets. On the outlet end, outflow boundary is applied for heat transfer physics and zero pressure is applied for the fluid flow physics. Non-slip boundary condition is applied to all boundaries. Insulation boundary condition is applied to the exterior walls and thermally thin approximation is applied to the interior wall (TPMS) with wall thickness of 0.5 mm. Figure 7(b) shows the streamline color coded by temperature in the TPMS-HX. From the inlet or outlet view, a helical-fashion flow pattern can be clearly observed. On one hand, this unique flow pattern help reduce the thickness of the thermal boundary layer on TPMS and enhance heat transfer. On the other hand, the helical-fashion flow prevents dirt or particulates from attaching to the TPMS and hence extends the serving life of the TPMS-HX.

Figure 8 shows the evolution of velocity in the first two periodic lengths of the TPMS-HX. The velocity pattern is taken from the cross-section of yz plane along the x axis when the flow reaches steady state. The flow velocity is significantly higher along the straight channels in the principle orientation as shown in Fig. 5(a). The velocity at the center of the straight channel is up to 50 mm/s, five times of the inlet velocity. The flow away from the center of the straight channel follows the surface gradient of the TPMS, spins about the center of the straight channel as moving forward, and eventually forms the helical-fashion flow. In addition, the velocity distribution is eccentric about the center of the straight channel as highlighted in Fig. 8, and the eccentric direction changes in counter-clockwise direction for this TPMS-HX design. By comparing velocity pattern at the same position of the first and second TPMS unit, one can observe that the flow is fully developed in the first periodic length.

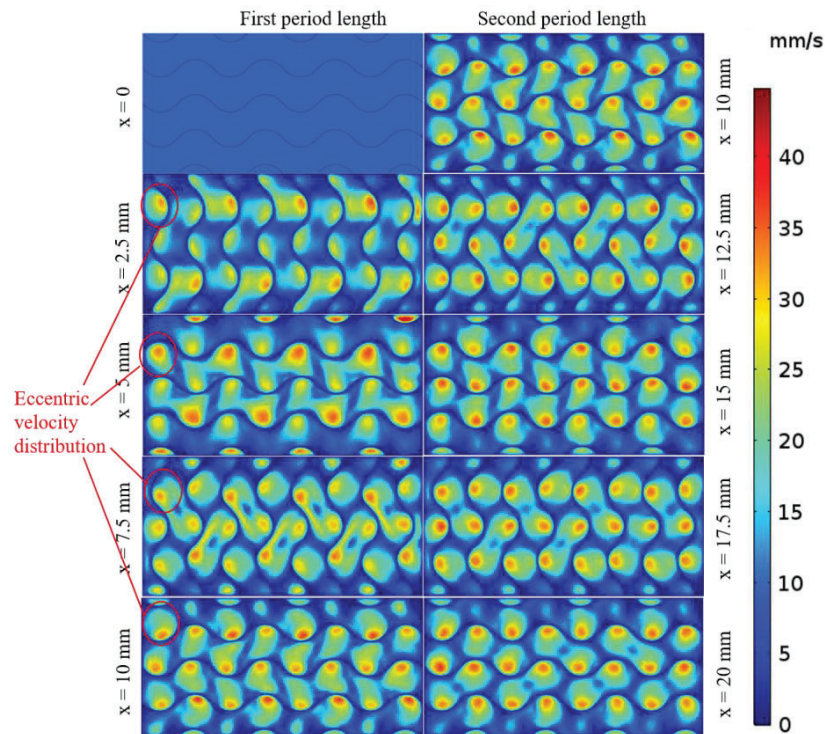


Figure 8. Evolution of flow velocity in the first two periodic length of the TPMS-HX.

3.3 Heat Transfer in TPMS-HX

Figure 9 shows the temperature evolution in the TPMS-HX. The hot flow is 100 °C and the cold flow is 20 °C at the inlet. After one periodic length ($x=10$ mm), the temperature of the cold and hot flow changes significantly, especially the flow away from the center of the straight channels. At the outlet ($x=100$ mm), the mixing-cup temperature of the hot and cold temperatures are 62.3 °C and 57.8 °C, respectively. The mixing-cup temperature is calculated with

$$T_{mixing-cup} = \frac{\int_D \rho C_p T \mathbf{u} \cdot \mathbf{n} ds}{\int_D \rho C_p \mathbf{u} \cdot \mathbf{n} ds} \quad (5)$$

where D is the surface area of the flow at outlet, \mathbf{u} is flow velocity at outlet and \mathbf{n} is the normal direction on outlet surface.

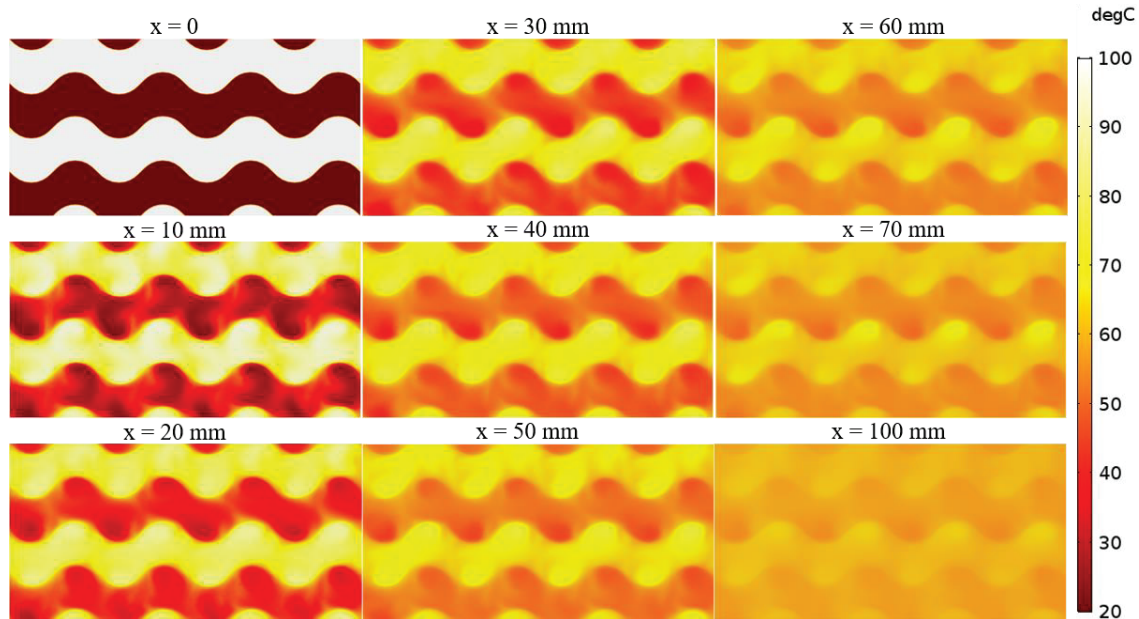


Figure 9. Evolution of temperature in the TPMS-HX.

To show the efficiency of the TPMS-HX, the TPMS-HX is benchmarked against a traditional plate heat exchanger with straight channels. The dimensions of the traditional heat exchanger are the same as the TPMS-HX. Two hot flow domains are sandwiched with two cold flow domains to resemble the flow condition in the TPMS-HX. Figure 10 shows the comparison of those two types of heat exchanger at inlet velocity of 10 mm/s and 20 mm/s. The interfacial surface area between the cold and hot flow is 251.5 cm² in TPMS-HX and 120 cm² in the reference heat exchanger as shown in Fig. 10(a). At the outlet, the mixing-cup temperature is significantly different for those two types of heat exchangers as shown in Fig. 10(b). The hot and cold fluid temperatures in TPMS-HX are much closer, showing a difference of 4.5 °C for inlet velocity of 10 mm/s and 7.9 °C for inlet velocity of 20 mm/s, as opposed to a difference of 42.4 °C for inlet velocity of 10 mm/s and 52.5 °C for inlet velocity of 20 mm/s in the reference heat exchanger. This is due to the high heat transfer rate in TPMS-HX. Figure 10(c) shows the maximum pressure drop. The pressure drop in TPMS-HX is also much higher than that in the reference heat exchanger. Maximum pressure drop in TPMS-HX with inlet velocity of 20 mm/s is 19.15 Pa while the counterpart in the reference heat exchanger is only 1 Pa. Figure 10(d) and 10(e) shows the comparison of heat transfer rate and heat transfer coefficients. Heat transfer coefficients are calculated as

$$h = \frac{P}{A(T_{hot} - T_{cold})}, \quad (6)$$

where P is the total exchanger power and A is the surface area through which P flows through. The heat transfer rates in the TPMS-HX are 630.9 W with inlet velocity of 10 mm/s and 1189.2 W with inlet velocity of 20 mm/s, 5.4 times and 7.5 times of their counterpart in the reference heat exchanger respectively. The heat transfer coefficients in the TPMS-HX are 313.5 W/(m²K) and 591 W/(m²K) for inlet velocity of 10 mm/s and 20 mm/s, respectively, showing an enhancement of 35.4% and 88.5% in comparison to the reference heat exchanger.

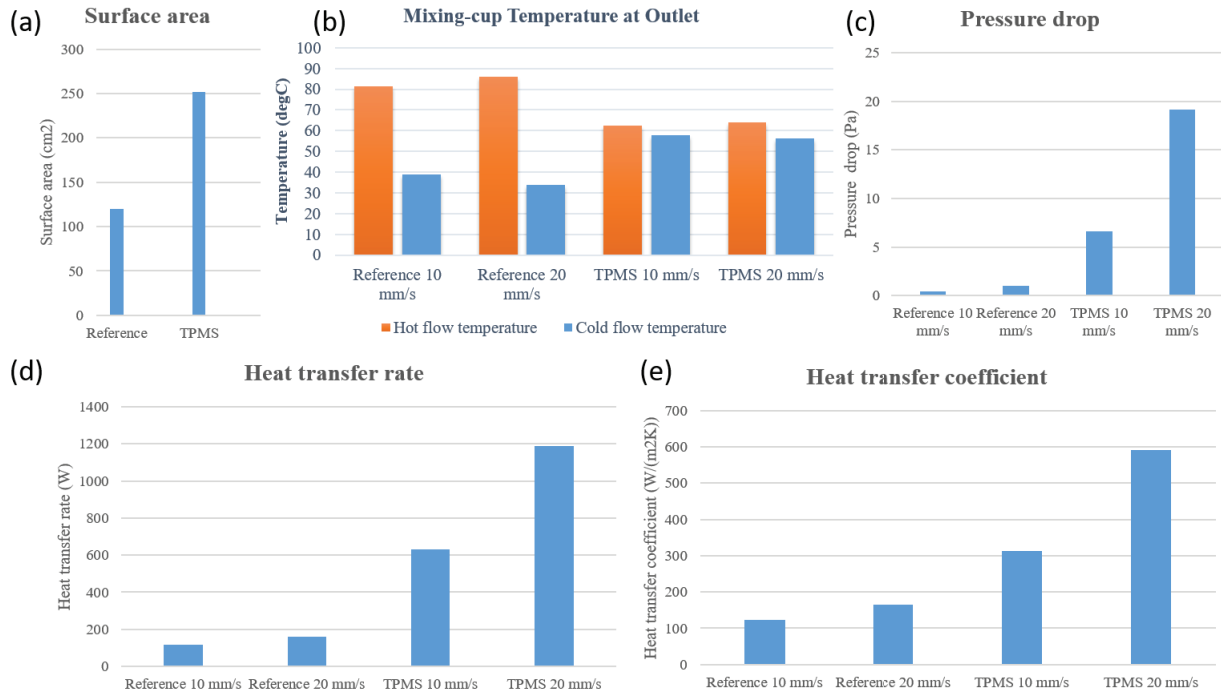


Figure 10. Comparison of the performance of TPMS-HX to a traditional plate heat exchanger.

Manufacturing of TPMS-HX with AM

4.1 TPMS-HX with AM

Figure 11 shows a TPMS-HX design and the cut-view of the design. The core of the TPMS-HX is a gyroid TPMS with wall thickness of 1 mm. In addition, boundary walls, inlets and outlets needs to be added to the TPMS to properly separate the hot and cold fluid. The TPMS-HX design was then imported to Atlas3D[®] (<https://atlas3d.xyz/>) to find a proper build orientation and generate necessary support structures as shown in Fig. 12(a). Atlas3D[®] is a cloud-based platform for optimizing build orientation and generating support structures for parts in AM. The oriented STL and support files were directly downloaded from Atlas3D[®] and imported to EOSPRINT. EOS M290 machine was employed to fabricate the TPMS-HX. The laser power is 220.1 W, laser scanning speed is 755.5 mm/s and the hatch distance is 110 microns. Metal powder feedstock 17-4PH stainless steel was used and 40 micron build layer was chosen. Figure 12(b) shows the final product of the TPMS-HX.

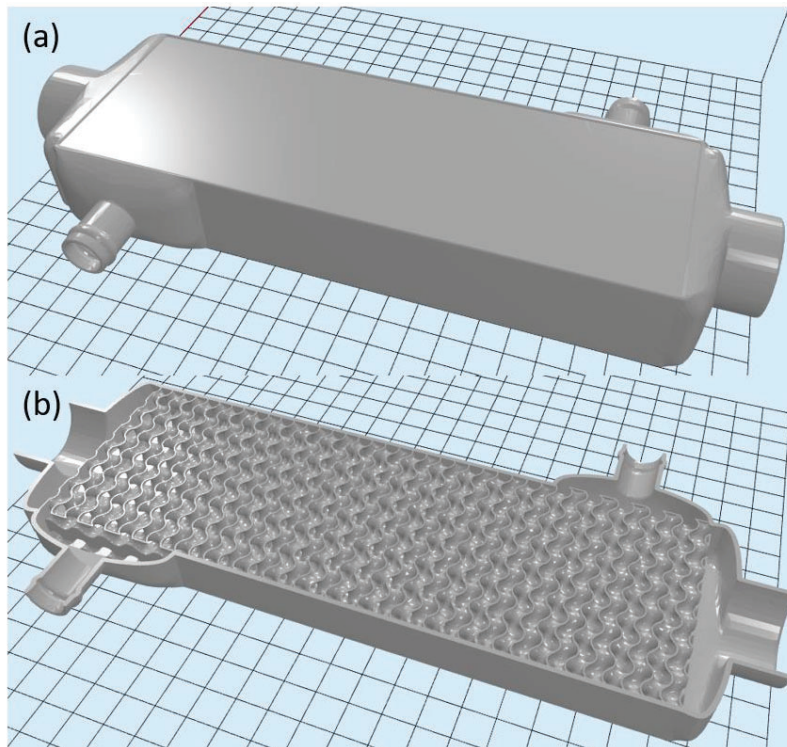


Figure 11. (a) TPMS-HX design. (b) Cut-view of the TPMS-HX design.

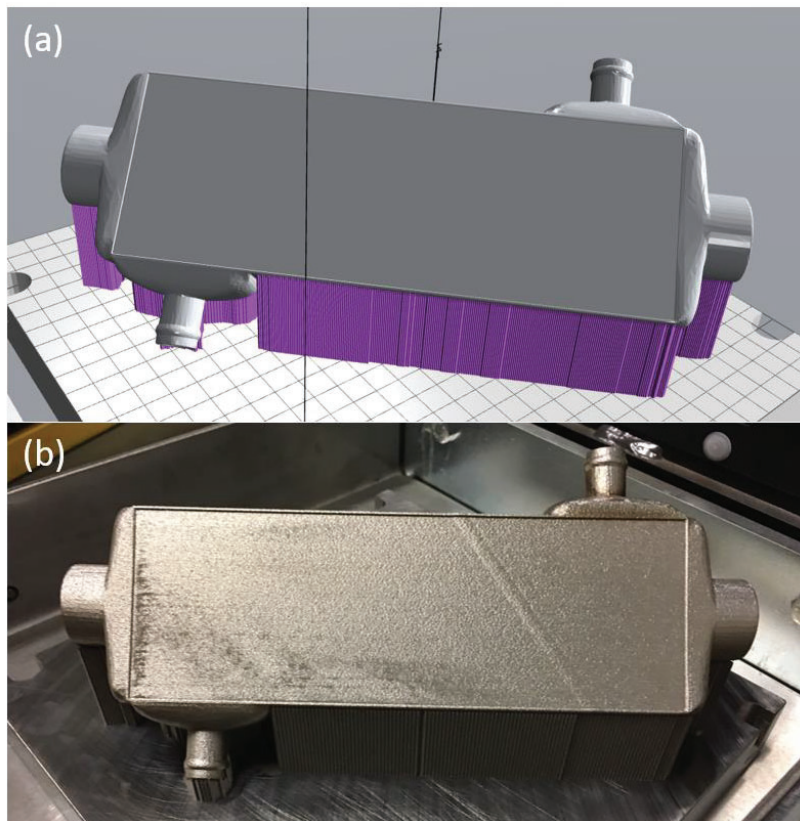


Figure 12 (a) TPMS-HX and its support structures in Atlas3D viewer. (b) TPMS-HX printed with EOS M290 machine.

4.2 Manufacturability of TPMS-HX by AM

Figure 13 shows a TPMS-HX with periodic length of 10 mm and wall thickness of 0.2 mm printed with a layer thickness of 40 microns in an EOS M290 machine. The TPMS-HX failed in leak test and after cutting the TPMS-HX with electrical discharge machining (EDM), a uniform distribution of voids on the TPMS can be observed. Those voids were probably due lack of fusion and were avoided by increasing the wall thickness to 1 mm in the new design. Influential factors on manufacturability of TPMSs include the types of triply periodic minimal surface, periodic length, wall thickness, build orientation and etc. The periodic length of the TPMS should be within a threshold so that heat at overhanging regions of TPMSs can dissipate efficiently. Small wall thickness is desired to reduce thermal resistance. However, strength and integrity of TPMSs also decreases with decreasing wall thickness.

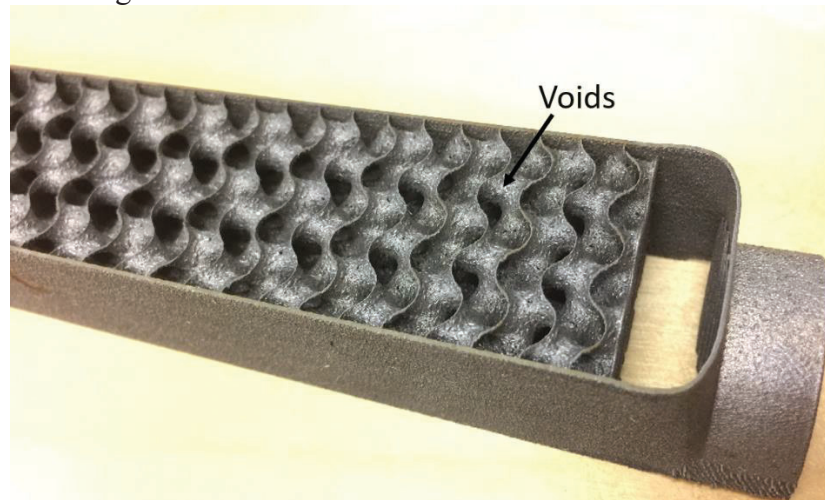


Figure 13. A TPMS-HX failed on leaking test due to voids on the TPMS.

Conclusion

In this study we proposed a novel heat exchanger design by utilizing the TPMS. The performance of the heat exchanger was demonstrated by developing a CFD model in COMSOL. Simulation results showed that heat transfer rates were improved by a factor of 7.5 times in comparison to a traditional plate heat exchanger. Finally, an industrial-size TPMS-HX was printed with an EOS M290 DMLS machine and manufacturability study on the TPMS-HX showed that a wall thickness larger than 0.2 mm was desired.

References

1. Ohadi, M., et al., *Recent Developments in High Temperature Heat Exchangers: A Review*. Frontiers in Heat and Mass Transfer, 2018. **11**.
2. Li, Q., et al., *Compact heat exchangers: A review and future applications for a new generation of high temperature solar receivers*. Renewable and Sustainable Energy Reviews, 2011. **15**(9): p. 4855-4875.
3. Southall, D., R.L. Pierres, and S.J. Dewson. *Design Considerations for Compact Heat Exchangers*. in *Proceedings of the 2008 International Congress on Advances in Nuclear Power Plants 2008*. Anaheim, CA USA.
4. Gibson, I., D.W. Rosen, and B. Stucker, *Additive Manufacturing Technologies: Rapid Prototyping to Direct Digital Manufacturing*. 2009: Springer US.

5. Gu, D.D., et al., *Laser additive manufacturing of metallic components: materials, processes and mechanisms*. International Materials Reviews, 2012. **57**(3): p. 133-164.
6. Neugebauer, R., et al., *Additive manufacturing boosts efficiency of heat transfer components*. Assembly Automation, 2011. **31**(4): p. 344-347.
7. *Heat exchanger designed by EOS*
https://www.eos.info/industries_markets/industry/other_industrial_applications.
8. Slaughter, V.B., *Method of using triply periodic minimal surfaces and minimal skeletons to make heat exchanger components* 2006, Boeing Co: US.
9. Ryan, R.C., *Triply periodic minimal surface area mass and heat transfer packing* 2013, GEOSPEAA LLC US.
10. Nguyen, D.T., et al. *Triply periodic triply periodic minimal surface heat exchangers for supercritical CO2 cycles*. in *Greenhouse Gas Control Technologies Conference*. 2018. Melbourne, Australia.
11. Chandrasekaran, G., *3D Printed Heat Exchangers An Experimental Study*, in *Mechanical Engineering*. 2018, Arizona State University.
12. Michielsen, K. and J.S. Kole, *Photonic band gaps in materials with triply periodic surfaces and related tubular structures*. Physical Review B, 2003. **68**(11): p. 115107.
13. Strano, G., et al., *A new approach to the design and optimisation of support structures in additive manufacturing*. The International Journal of Advanced Manufacturing Technology, 2013. **66**(9-12): p. 1247-1254.